VOLCANICA Article in Press

Ripa Khodijah, Suci Ramayanti, Andi Suhandi, Chang-Wook Lee and Nanang Dwi Ardi (2026) "Lagged Relationships Between Volcanic SO_2 Emissions and Local Weather Parameters in the Aftermath of the 2024 Mount Lewotobi Laki-laki Eruption", *Volcanica*, 9(2). doi: 10.30909/vol/yjtk2483.

Lagged Relationships Between Volcanic SO_2 Emissions and Local Weather Parameters in the Aftermath of the 2024 Mount Lewotobi Laki-Laki Eruption

Abstract

The Indonesian Volcanology and Geological Hazard Mitigation Centre (PVMBG) has raised the status of Mount Lewotobi Laki-Laki to Level IV (AWAS), accompanied by massive eruptive activity with sulphur dioxide (SO_2) emissions exceeding 10,000 tons/day and an eruption column about 8,000 meters high. This activity may affect local weather parameters, including surface temperature, sulphate aerosol concentration, cloud optical thickness (COT), and precipitation. To identify the influence, this study applies cross-correlation function (CCF) analysis using multi sensor satellite data (OMI, AIRS, MERRA-2, MODIS, GPM). The analysis showed positive correlations with time lags: surface temperature responded after 1 day with $r = 0.50$, sulphate aerosol after 16 days with $r = 0.62$, cloud optical thickness after 21 days with $r = 0.39$, and precipitation after 23 days with $r = 0.55$. These findings demonstrate the influence of SO_2 emissions on local weather and provide valuable insights for mitigation in active regions.

Keywords

Mount Lewotobi Laki-Laki; SO_2 emissions; Local Weather; Lag Time; Satellite Data.

Non- Technical Summary

Mount Lewotobi Laki-Laki in Flores, Indonesia, is currently experiencing an increase in volcanic activity and is at the highest alert level (AWAS). Satellites observed amounts of sulphur dioxide (SO_2) gas and towering ash columns. We analysed satellite data to evaluate the influence of volcanic SO_2 emissions on local weather, including surface temperature, sulphate aerosols, cloud optical thickness, and precipitation. We found that the SO_2 increase was indeed associated with these weather changes. However, the impacts occur with a lag of days to weeks. These findings suggest that volcanic eruptions can affect weather conditions in volcanically active regions.

Keywords

Mount Lewotobi Laki-Laki; SO_2 emission ; Local weather; Satellite Observations; lag of days.

1. Introduction

Volcanic activity, as a dynamic manifestation of Earth's internal processes, exerts a profound influence on the global atmosphere. Beyond ejecting pyroclastic materials and lava, volcanoes emit substantial quantities of gases, particularly sulphur dioxide (SO_2) (Schallock et al., 2023; Yu et al., 2023). The injection of SO_2 into the atmosphere, especially during explosive eruptions, is one of the main precursors to the formation of sulphate aerosols (Marshall et al., 2020; Sellitto et al., 2024). These aerosols play an important role in influencing weather and climate through radiative mechanisms and cloud microphysics (Sahoo, 2024; Toohey et al., 2021). Their radiative impact, especially at shortwave, can cause surface cooling (Lacis et al., 2013; Stenchikov, 2009), modulate convective processes (Ceppi et al., 2017), and disrupt large-scale circulation patterns (Su et al., 2024; Timmreck et al., 2021).

While the climatic implications of volcanic sulphate aerosols are often discussed in a global over timescales of months to years (Hermanson et al., 2020), growing evidence indicates that the most immediate atmospheric responses to volcanic SO_2 occur within the troposphere following its release. Observations across diverse volcanic systems reveal that tropospheric SO_2 exhibits strong sub daily to short term variability. This variability demonstrates that rapid atmospheric processing serves as a dominant short-term mechanism. Furthermore, these immediate effects operate independently of the longer-term climate impact (Arellano et al., 2021; Haghighatnasab et al., 2022). Modelling studies further demonstrate that SO_2 injected into the mid to lower troposphere is efficiently converted into sulphate aerosols through gas-phase oxidation pathways, underscoring the importance of tropospheric chemical transformation (Hagen et al., 2023; Haghighatnasab et al., 2022). The resulting enhancement in tropospheric aerosol loading substantially increases cloud droplet number concentrations, strengthening aerosol cloud interactions and modifying cloud optical properties and precipitation efficiency in the lower atmosphere (Fan et al., 2018). These processes operate on short temporal scales and are highly sensitive to local meteorological conditions, particularly in tropical environments dominated by convection and strong moisture variability (Amiot et al., 2025; Reid et al., 2023).

Although the global climate impacts of significant volcanic eruptions have been widely studied (Stenchikov, 2009; Stenchikov et al., 2002), regional atmospheric influences on the tropics remain insufficiently understood. This gap is particularly apparent in the Lesser Sunda islands, an archipelago characterized by complex topography, monsoonal circulation, and strong ocean-atmosphere interactions (Mahrup et al., 2021; Simanjuntak et al., 2022; Wirasatriya et al., 2021). Disturbances from elevated SO_2 and subsequent sulphate aerosol formation can interact with local humidity, sea surface temperature, and seasonal wind patterns, affecting precipitation and convective dynamics (Li et al., 2016; Sadeghi et al., 2025; Whitty et al., 2020).

Recent studies have shown that sulphate aerosols not only increase cloud albedo and cause surface cooling, but also trigger dynamic feedbacks such as changes in latent heat release and regional circulation (Chen et al., 2024; Virtanen et al., 2025; Zheng et al., 2024). These effects often appear with a time lag, suggesting the existence of an integrated process involving cloud microphysics and atmospheric boundary layer dynamics adjustments (Axebrink et al., 2025; Sellitto et al., 2024). However, empirical quantification of the lag relationship between volcanic SO_2 and atmospheric variables such as surface temperature, sulphate aerosols, cloud optical thickness (COT), and precipitation is scarce, especially in tropical island environments.

The recent eruption of Mount Lewotobi Laki-Laki (November 2024) provides an ideal natural study site to analyse this phenomenon. On November 3, 2024, the PVMBG raised the alert status to Level IV (AWAS) after an eruption that spewed an ash column 8 km high and released more than 10,000 tons/day of SO_2 (Ministry of Energy and Mineral Resources., 2024a, 2024b). This high SO_2 flux has the potential to disrupt regional weather conditions, triggering a two-phase thermal response: an initial warming phase through radiation absorption followed by a delayed cooling phase due to increased cloud cover and altering precipitation patterns through microphysical mechanisms and atmospheric dynamics (Lin et al., 2025; Malavelle et al., 2017; Marshall et al., 2022; Paik et al., 2023).

Most previous studies have focused on global climate modelling. Few studies have utilized a statistical framework to detect the lagged atmospheric response of volcanic SO_2 disturbances. Findings from an urban air pollution study show that SO_2 has significant delayed correlations with surface temperature (positive at +3, +5, +13, and +16 days) and with precipitation (negative after +1 day) (Liu et al., 2025). Although providing valuable insights, this approach has had limited application in volcanic studies on tropical islands.

To address this gap, the study integrates multi-satellite observations with Cross Correlation Function (CCF) analysis to quantify the temporal and spatial linkages between volcanic SO_2 and key weather variables in the Lesser Sundas. In particular, it detects lag-dependent sequential associations between SO_2, sulphate aerosols, COT, surface temperature, and precipitation, and visualizes the spatial heterogeneity of atmospheric response following volcanic SO_2 emissions. This integrative framework provides new insights into the short-term atmospheric impacts of volcanic SO_2, improves regional weather understanding, and supports disaster risk mitigation strategies.

2. Data and Methodology

This study employs an integrated framework of satellite-based observations and statistical analysis to assess the atmospheric response to volcanic SO_2 emissions from the Laki-Laki Mount Lewotobi. Daily datasets from OMI, AIRIS, MERRA-2, MODIS, and GPM underwent preprocessing through noise filtering and temporal resampling to obtain consistent daily resolution. We employed cross-correlation function (CCF) analysis to quantify the lag-dependent associations between SO_2, surface temperature, sulphate aerosol, cloud optical thickness (COT), and precipitation. This approach enables systematic detection of sequential atmospheric responses, while providing new insights into the timing and intensity of aerosol, cloud, and precipitation interactions following volcanic emissions. The methodological workflow is summarized in Figure 1, which highlights the stages from raw satellite data acquisition to final interpretation in the temporal and spatial domains.

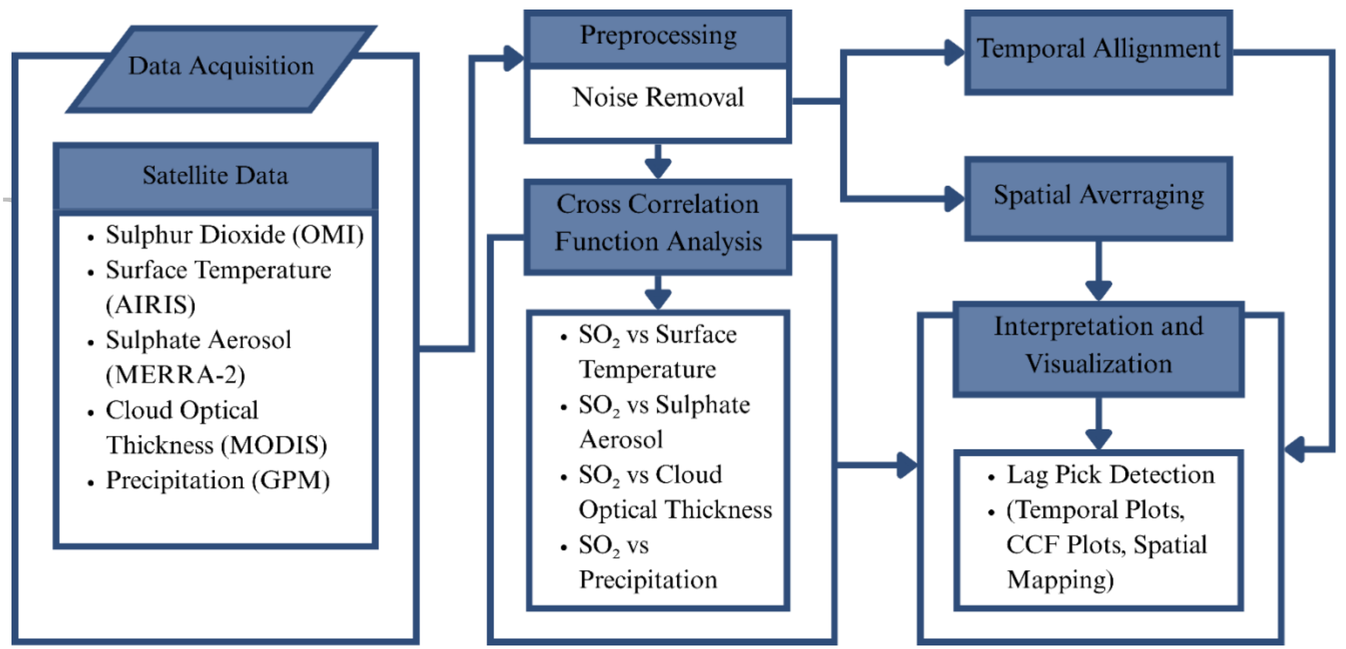

Figure 1. Flowchart of the methodology illustrating the analytical framework of the study, starting with the acquisition of satellite data (SO_2, temperature, aerosols, COT, and precipitation), followed by the process of data filtering (noise removal) and temporal alignment, Cross-Correlation Function (CCF) analysis on weather variables, and ending with temporal interpretation and spatial visualization.

2.1 Data Acquisition

This study examines the atmospheric impact of post-eruption volcanic SO_2 emissions of Mount Lewotobi Laki-Laki by analysing datasets extracted from various satellite instruments via the Giovanni platform (https://giovanni.gsfc.nasa.gov/). The total SO_2 column, which serves as the independent variable, was obtained from the Ozone Monitoring Instrument (OMI) operating on the Aura satellite (https://aura.gsfc.nasa.gov/omi.html). The dependent variable is the surface temperature of the lower troposphere, which was obtained from the Atmospheric Infrared Sounder (AIRS) on the Aqua satellite (https://airs.jpl.nasa.gov/). Sulphate aerosol concentrations were derived via the MERRA-2 reanalysis product (https://gmao.gsfc.nasa.gov/reanalysis/MERRA-2/). Cloud Optical Thickness (COT) data were retrieved from the Moderate Resolution Imaging Spectroradiometer (MODIS) instrument on the Aqua and Terra satellites (https://modis.gsfc.nasa.gov/). Daily precipitation data were sourced from the Global Precipitation Measurement (GPM) mission a collaboration between NASA and JAXA (https://gpm.nasa.gov/). The analysis period spans 1 October to 31 December, 2024, allowing for a comprehensive assessment of weather conditions before, during, and after the eruption.

2.2 Study Area

This study focuses on the Lesser Sunda Islands, an active volcanic archipelago in eastern Indonesia spanning a total land area approximately 75,000 km^2. The region includes the main islands of Flores, Sumba, Timor, Savu, and Lembata, along with their surrounding marine environments. It is bordered by the Banda Sea to the north, the Savu Sea to the south, and the Flores Sea and Timor Sea to the east and west (Mahrup et al., 2021). A spatial overview of the study site, illustrating the position of Mount Lewotobi Laki-Laki and the geographic setting of the Lesser Sunda Islands, is presented in Figure 2.

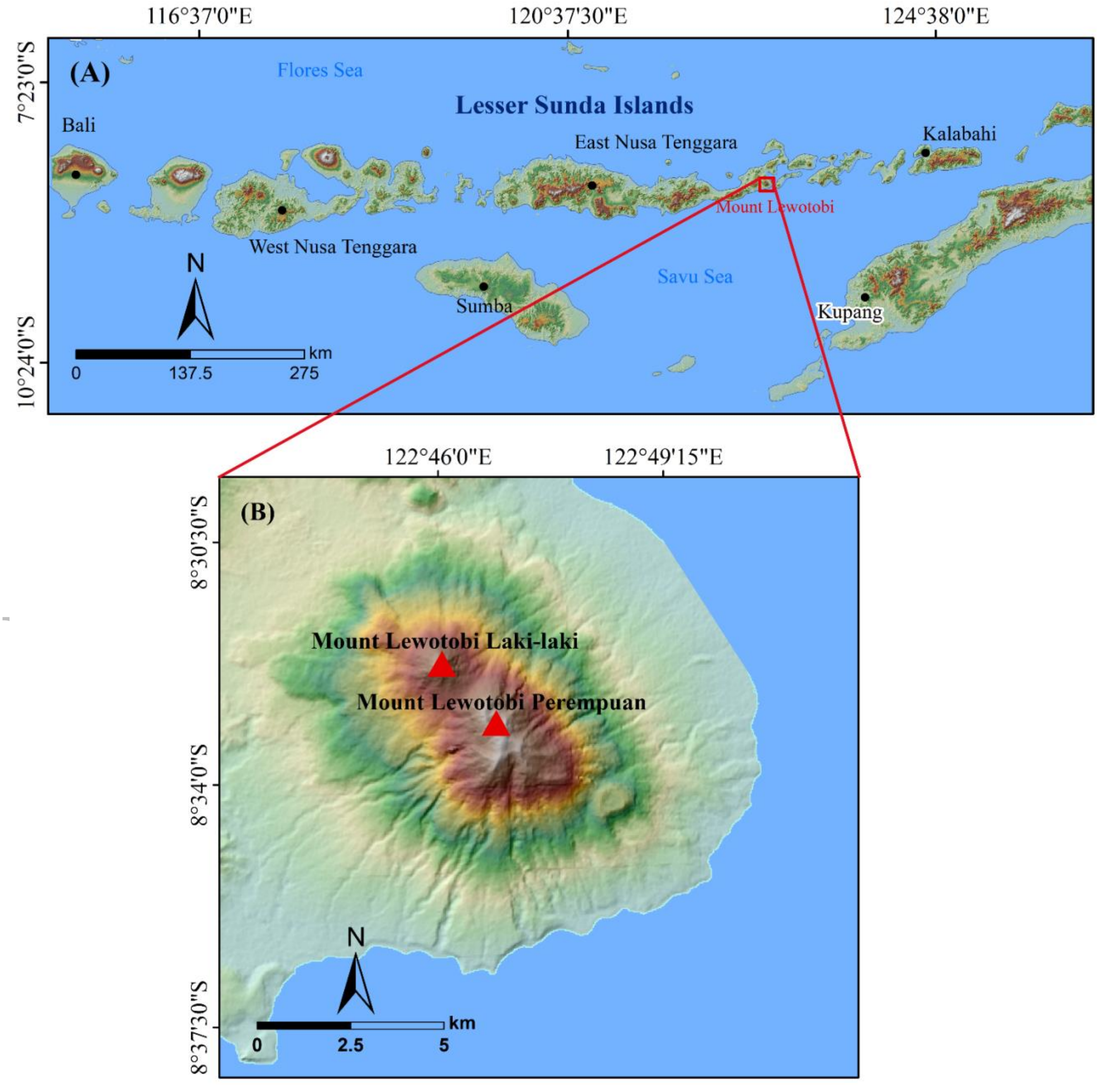

135 **Figure 2.** (A) Geographical location of the Lesser Sunda Islands, including the mainland and surrounding seas; (B) Position of Mount Lewotobi Laki-Laki and Mount Lewotobi Perempuan.

The Lesser Sunda region experiences a tropical monsoon climate has driven by the Asia-Australia monsoon system. During the wet season (October - April), north-westerly winds transport moisture from the Indian and Pacific Oceans. In contrast, dry easterlies from mainland Australia dominate the dry season (May - September) (Trismidianto et al., 2024). Mean annual temperatures range between 26 °C and 28 °C, with substantial precipitation variability. Recent climatological analyses indicate a decline in precipitation linked to rising sea surface temperatures (Mahrup et al., 2021). Furthermore, previous studies in Indonesia have demonstrated that large-scale atmospheric phenomena such as tropical cyclones can significantly alter local meteorological parameters, including temperature, pressure, and humidity (Nugroho et al., 2019), underscoring the sensitivity of the regional climate system to external forcings.

Topographically, the region consists of rugged volcanic mountains, steep coastal slopes, and limited lowlands. Mount Lewotobi Laki-Laki (1,584 m a.s.l.) and Mount Lewotobi Perempuan (1,703 m a.s.l.) are paired active volcanoes in East Flores (Global Volcanism Program, 2024), forming part of the Sunda Arc, a subduction-related volcanic chain generated by the convergence of the Indo-Australian and Eurasian plates (Hall, 2012). Oceanographically, the region is subject to seasonal upwelling and the Indonesian Throughflow, which regulates local sea surface temperatures and can affect post-eruption aerosol dispersion (Wirasatriya et al., 2021). The interactions between volcanic activity, monsoon circulation, and the complex topography of the islands make this an ideal region to evaluate the influence of volcanic SO_2 emissions on local weather dynamics through lag correlation analysis using the Cross-Correlation Function (CCF).

2.3 Cross-Correlation Function (CCF) analysis

The primary analysis in this study uses the Cross-Correlation Function (CCF) to evaluate the temporal relationship between volcanic SO_2 emissions and local weather variables, including surface temperature, sulphate aerosol, cloud optical thickness (COT), and precipitation. The CCF calculates the Pearson correlation coefficient (r) between the SO_2 time series and each local weather parameter at various lags (τ), thereby identifying the strength and direction of the delayed relationship. The r value at each lag was interpreted using Papageorgiou (2022) classification: $r > 0.9$ (almost perfect), $0.7 < r \leq 0.9$ (very strong), $0.5 < r \leq 0.7$ (strong), $0.3 < r \leq 0.5$ (moderate), $0.1 < r \leq 0.3$ (weak), and $r < 0.1$ (very weak). Mathematically, the CCF for two discrete time series, $x\ (t)$ and $y\ (t)$, at lag τ is defined as:

$$CCF = \frac{\sum_{t=1}^{N-1}[(x(t) - \bar{x}) * (y(t - lag) - \bar{y})]}{\sqrt{\sum_{t=1}^{N-1}(x(t) = \bar{x})^2 \sum_{t=1}^{N-1}(y(t - lag) - \bar{y})^2}} \quad (1)$$

where, $\bar{x}$ and $\bar{y}$ are the mean values and N is the number of observations (Hoffmann et al., 2024). The lag with the highest correlation coefficient (r) indicates the time lag of the atmospheric response to peak SO_2 emissions. A positive correlation reflects an increase in weather variables concurrent with rising SO_2 emissions, while a negative correlation signifies an inverse response.

3. Results

3.1. Daily Observations of SO_2 Emissions and Weather Parameters

Daily observations of the atmospheric response were analysed by representing daily values spatially averaged over a fixed regional domain (115°-125°E, 11°-8°S). This specific domain was selected to encompass Mount Lewotobi and its dominant downwind transport pathway under prevailing monsoonal circulation, ensuring that the non-stationary nature of the SO_2 plume was captured within the study area. Furthermore, the analysis was systematically segmented into three temporal phases to provide a consistent atmospheric framework: the pre-eruption period (1 October - 2 November), the eruption phase (3 November - 3 December), and the post-eruption period (4-31 December). During the eruptive phase, SO_2 concentrations exhibited a sharp increase, peaking at approximately 50.62 kt (Figure 3A). This abrupt rise triggered a sequence of atmospheric responses. During the eruption, surface temperatures initially climbed to about 27.6 °C (Figure 3B), likely driven by direct radiative heating from volcanic gas emissions and particle interactions in the atmosphere. Following the emission peak, temperatures did not immediately return to baseline but gradually declined to approximately 25.0 °C in the post-eruption period (Figure 3B). This pattern reflects a two-stage thermal response: initial warming followed by delayed cooling, mediated by the formation of sulphate aerosols.

Sulphate aerosol concentrations began to increase several days after the SO_2 peak, and reached a maximum of 1.7×10^{-5} kg/m^2 (Figure 3C). This delay reflects the time required for the chemical reaction of SO_2 oxidation in the atmosphere, and confirms that sulphate aerosols have a longer residence time in the atmosphere. These aerosols also affected cloud properties, as evidenced by a substantial increase in Cloud Optical Thickness (COT), which peaked at 22.1 (Figure 3D), substantially higher than the pre-eruption daily range of 5-10. This increase is in line with the Twomey effect, where the number of small cloud droplets increases as sulphate aerosols act as cloud condensation nuclei (CCN), resulting in thicker and more reflective clouds. Even after SO_2 emissions decreased, COT values remained high for several days before returning to normal, confirming the role of persistent aerosols in modifying cloud structure.

Meanwhile, precipitation exhibited an opposite trend. Before the eruption, daily precipitation was relatively low, averaging 0-4 mm/day, with a brief spike of approximately 28 mm/day in late October, likely marking the onset of the Lesser Sunda rainy season (Mahrup et al., 2021). During the eruptive phase, precipitation declined sharply to 0-5 mm/day and occasionally dropped to near zero, despite otherwise favorable atmospheric conditions for cloud formation. This pattern suggests a disruption of raindrop coalescence caused by elevated concentrations of sulphate aerosols acting as CCN. Following the decline of SO_2 emissions, precipitation increased substantially, reaching a peak of ~38 mm/day in early December (Figure 3E). Such a sequence reflects a lagged hydrological response to volcanic SO_2 emissions, in which aerosol injection temporarily suppresses precipitation before intensification resumes as atmospheric conditions stabilize. The temporal evolution of this response is systematically illustrated in Figure 3 (A-E), highlighting the interconnections between SO_2 dynamics and key weather variables.

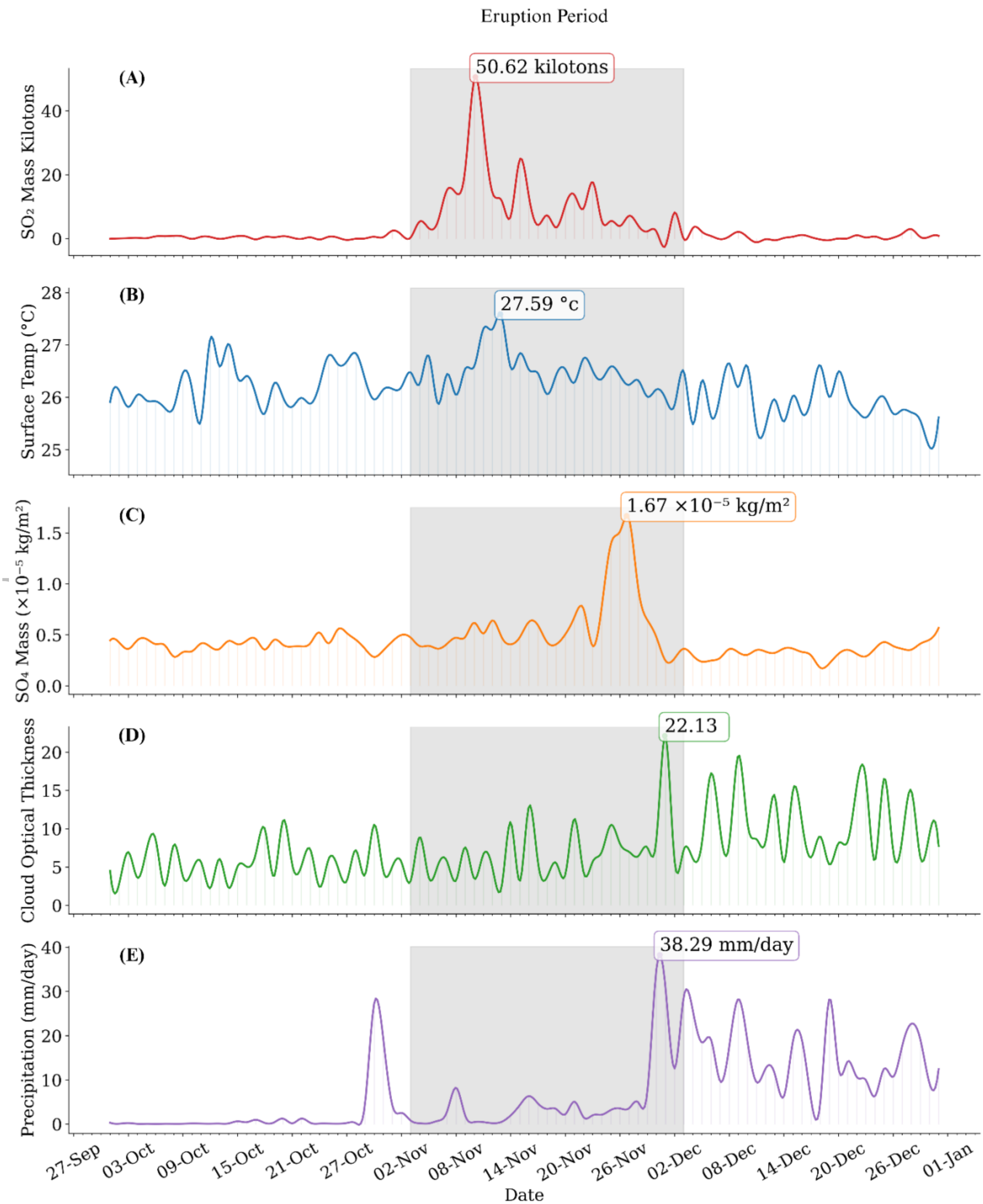

Eruption Period
(A)
50.62 kilotons
SO₂ Mass Kilotons
(B)
27.59 °c
Surface Temp (°C)
(C)
1.67 ×10⁻⁵ kg/m²
SO₄ Mass (×10⁻⁵ kg/m²)
(D)
22.13
Cloud Optical Thickness
(E)
38.29 mm/day
Precipitation (mm/day)
27-Sep
03-Oct
09-Oct
15-Oct
21-Oct
27-Oct
02-Nov
08-Nov
14-Nov
20-Nov
26-Nov
02-Dec
08-Dec
14-Dec
20-Dec
26-Dec
01-Jan
Date

Figure 3: Daily variations of SO_2 emissions (kiloton), and cuacalocal parameters including surface temperature (°C), SO_4 mass (×10^{-5} kg/m^2), cloud optical thickness (COT), and precipitation (mm/day). The gray area marks the eruption period (3 November - 3 ecember, 2024), which could potentially affect the observed atmospheric dynamics.

3.1 Responses: Cross-Correlation Analysis

Cross-correlation function (CCF) analysis between volcanic SO_2 emissions and atmospheric parameters reveals distinct temporal response patterns, reflecting the sequential nature of atmospheric processes triggered by eruptive activity. To establish a temporal baseline, the analysis utilizes the peak SO_2 emission observed on 10 November, 2024 (as shown in Figure 3A) as the reference point (lag = 0). In this context, the lag values represent the duration required for the eruptive peak to generate a maximum response or peak pattern in each meteorological parameter. The fastest response appears in surface temperature (Figure 4A), which reaches a maximum correlation of $r = 0.51$ at a 1-day lag (11 November). This finding indicates that SO_2 immediately affects the surface radiation balance, either through direct absorption of solar radiation or through initial interactions with cloud cover. After peaking, the correlation declines sharply and enters negative values between lags of 15-35 days, suggesting that the short-lived radiative effects of SO_2 are given way to by secondary processes, such as the formation of sulphate aerosols from atmospheric SO_2 oxidation, which can increase cloud albedo and reduce incoming solar radiation at the surface.

A subsequent response emerges in sulphate (SO_4) aerosols (Figure 4B), reaching a peak correlation of $r = 0.62$ at a 16-day lag (26 November). This delay aligns with the atmospheric conversion of SO_2 into secondary sulphate particles through oxidation processes. Once generated, these aerosols influence cloud microphysics, as evidenced by a peak in cloud optical thickness (COT) at day 21 (1 December), showing a correlation of $r = 0.39$ (Figure 4C). The rise in COT reflects an enhanced cloud droplet number and greater optical density, driven by the role of aerosols as cloud condensation nuclei (CCNs).

Precipitation exhibits the most delayed response (Figure 5D), reaching a peak correlation of $r = 0.55$ at a 23-day lag which closely matches the significant rainfall intensification observed on December 3 (Figure 3E). This behaviour aligns with the final stage of the aerosol-cloud-precipitation feedback cycle, in which modifications to cloud microphysics ultimately enhance precipitation efficiency. The progression of peaks spanning rapid radiative forcing, chemical transformation to aerosols, cloud adjustment, and precipitation modulation depicts a complete atmospheric pathway initiated by volcanic SO_2 emissions. This sequential relationship is clearly illustrated in Figure 5A-D.

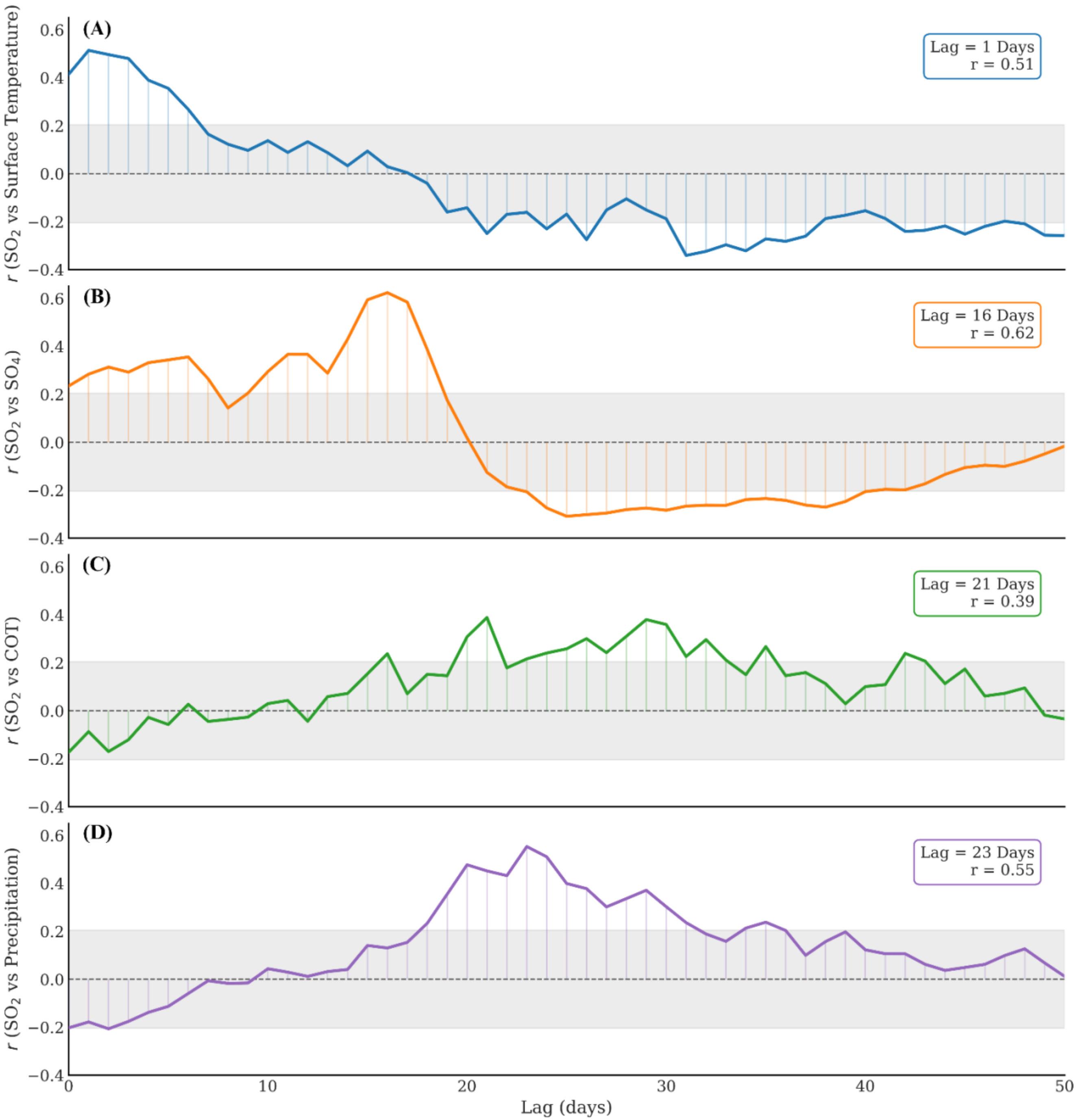

Figure 4. Cross-correlation analysis between volcanic SO_2 emissions and four local weather parameters: (A) surface temperature, (B) SO_4 aerosol, (C) cloud optical thickness (COT), and (D) precipitation, during the Mount Lewotobi Laki-Laki observation period 2024. The x-axis shows the time lag (lag, in days), where a positive lag indicates changes in SO_2 precede changes in the associated atmospheric parameters. Each panel displays the maximum correlation coefficient (r) along with its optimal lag, marked by the dashed vertical line and the highlighted dot. The Gray-shaded area represents the ±95% confidence interval, where correlation values within this range are statistically insignificant.

4. Discussions

Daily observations of surface temperature indicates that although the Lesser Sunda Islands experience dynamically varying daily temperature fluctuations, the peak of 27.59 °C recorded in November represents a pronounced thermal anomaly that spatially coincides with the eruptive activity of Mount Lewotobi (Figure 3B). This value is particularly significant as it exceeds the regional climatological baseline for the early wet season transition, which typically remains below 27.5 °C (Simanjuntak et al.,, 2022). Physically, this elevated temperature suggests an additional thermal energy input via the volcanic blanket effect, where volcanic gases and ash trap outgoing terrestrial longwave radiation (Sellitto et al., 2024). The robustness of this anomaly is further supported by the cross correlation function (CCF) analysis, which reveals a very short lag of only 1 day between SO_2 emissions and the observed temperature increase. Evidence of this localized energy enhancement is clearly illustrated in the November transect profile (Figure 6E), where the most pronounced temperature increase is concentrated specifically from the crater extending up to 3 km aestward, corresponding to the location of the eruption source.

However, as the eruption progresses, this warming phase is temporary. The subsequent gradual cooling toward ~25 °C during the later stages of the eruption period aligns with the peak accumulation of sulphate aerosols (Figure 3C), This ~25 °C stabilization is consistent with the climatological baseline for the Lesser Sunda Islands region during this transition, which typically ranges between 25 °C and 27.5 °C (Simanjuntak & Lin, 2022). This transition is driven by atmospheric chemical transformations where the initial thermal phase decays and promotes the formation of sulphate aerosols, reaching their maximum correlation at a 16-day ($r = 0.62$). This pattern reflects oxidation processes involving hydroxyl radicals (OH) under ultraviolet radiation, combined with the influence of ambient atmospheric humidity, consistent with the estimated e-folding lifetime of volcanic SO_2 of approximately 13-17 days (Cai et al., 2022). In response to the inherently non-stationary nature of volcanic plumes, spatial analysis (Figure 6.H) demonstrates that these aerosols do not remain confined above the crater but are transported by prevailing winds moving from east to west. The resulting accumulation of sulphate aerosols subsequently acts as a catalyst for cloud microphysical modification, leading to an increase in Cloud Optical Thickness (COT) with a 21-day lag (r = 0.39). This elevation in COT, despite the absence of immediate precipitation, indicates the formation of an optically dense yet meteorologically stable cloud layer, a phenomenon driven by the high concentration of volcanic aerosols. The conceptual framework for these microphysical modifications is further detailed in Figure 5.

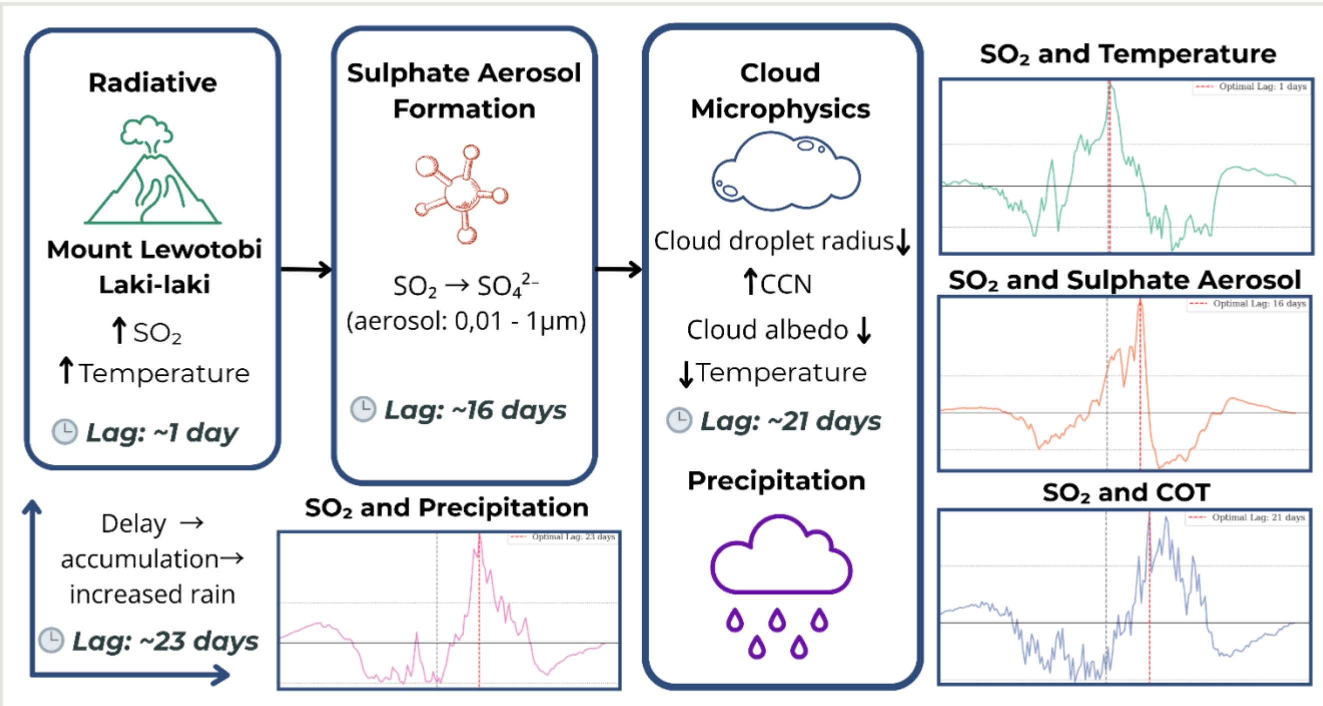

Figure 5. Conceptual diagram of cloud microphysical modifications. The illustration depicts the transition from SO_2 to sulphate aerosols acting as cloud condensation nuclei (CCN), promoting droplet competition and suppressed coalescence (Twomey effect), which increases COT without immediately producing precipitation.

From a microphysical perspective, the massive injection of fine aerosols (< 1 μm) intensifies competition for available water vapour, producing cloud droplets with high number concentrations but very small diameters, thereby inhibiting efficient coalescence processes. This mechanism explains the anomaly observed in Figure 3, where despite the region having already passed the natural monsoon onset during the final week of October (rainfall peak of ~28 mm day), precipitation throughout November was markedly suppressed, approaching near zero values. Under these conditions, water mass remained effectively suspended within the atmosphere, while air masses were advected from the crater source region (0 km) toward the downstream sector (0-33 km), as detailed in the conceptual framework in Figure 5.

The hydrological response ultimately reached a saturation point in December, when the accumulated atmospheric water mass was released as extreme precipitation reaching 38.29 mm/day. The observed 23-day lag represents the physical timescale required for the air mass to travel across the east to west transport pathway while undergoing progressive microphysical maturation. Unlike the sporadic rainfall events observed in October, the December precipitation burst was both intense and spatially displaced toward the 0-33 km sector (Figure 6O), reflecting the downwind transport pathways established during the peak SO_2 loading in November. This phenomenon provides clear evidence of an aerosol indirect effect, whereby interactions between volcanic emissions and atmospheric transport dynamics fundamentally altered the normal seasonal rainfall pattern, ultimately producing an extreme hydrometeorological response in the downwind region (Wong et al., 2025). Similar short-term meteorological anomalies have been documented following the 2022 Hunga Tonga-Hunga Ha'apai eruption, where a maturation period of several weeks was required for atmospheric cooling and cloud formation to culminate in record-breaking rainfall (Wong & Yim, 2022). Furthermore, our observed 23-day lag closely matches historical records where distal regions, such as Hong Kong, recorded precipitation delays of 23 to 35 days following the 1982 El Chichón and 2008 Chaitén eruptions (Wong et al., 2023; Yim, 2005). While the Tongan event reached stratospheric heights and involved massive water vapor, the Lewotobi Laki-Laki case demonstrates that tropospheric sulphur loading can trigger comparable physical maturation timescales, leading to similar downwind precipitation bursts. The synthesized relationship between these spatiotemporal variables is illustrated in the schematic and transect profiles in Figure 6.

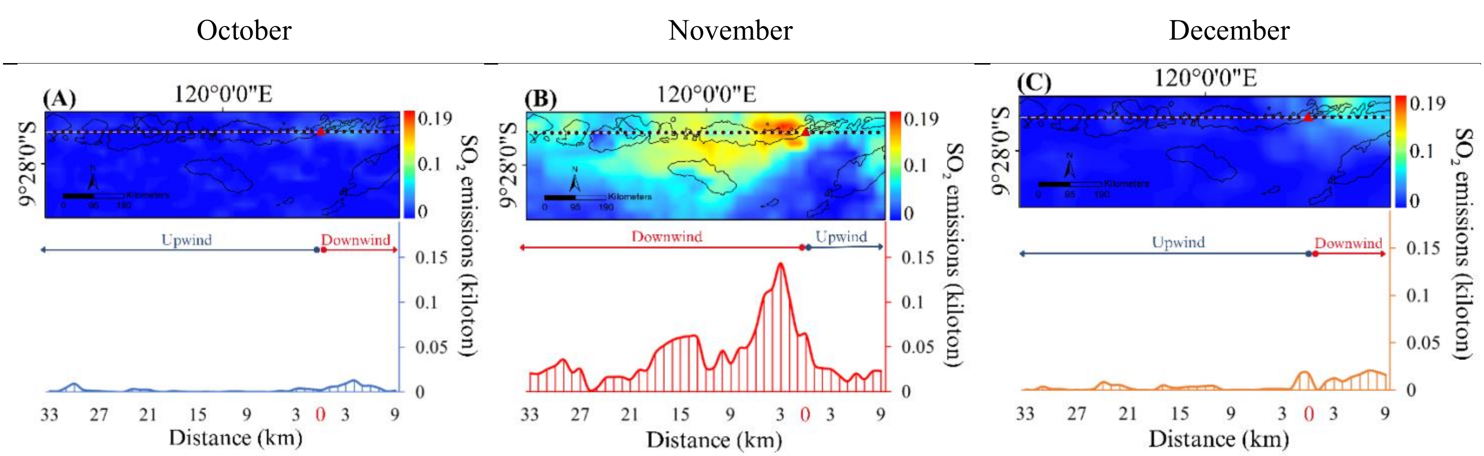

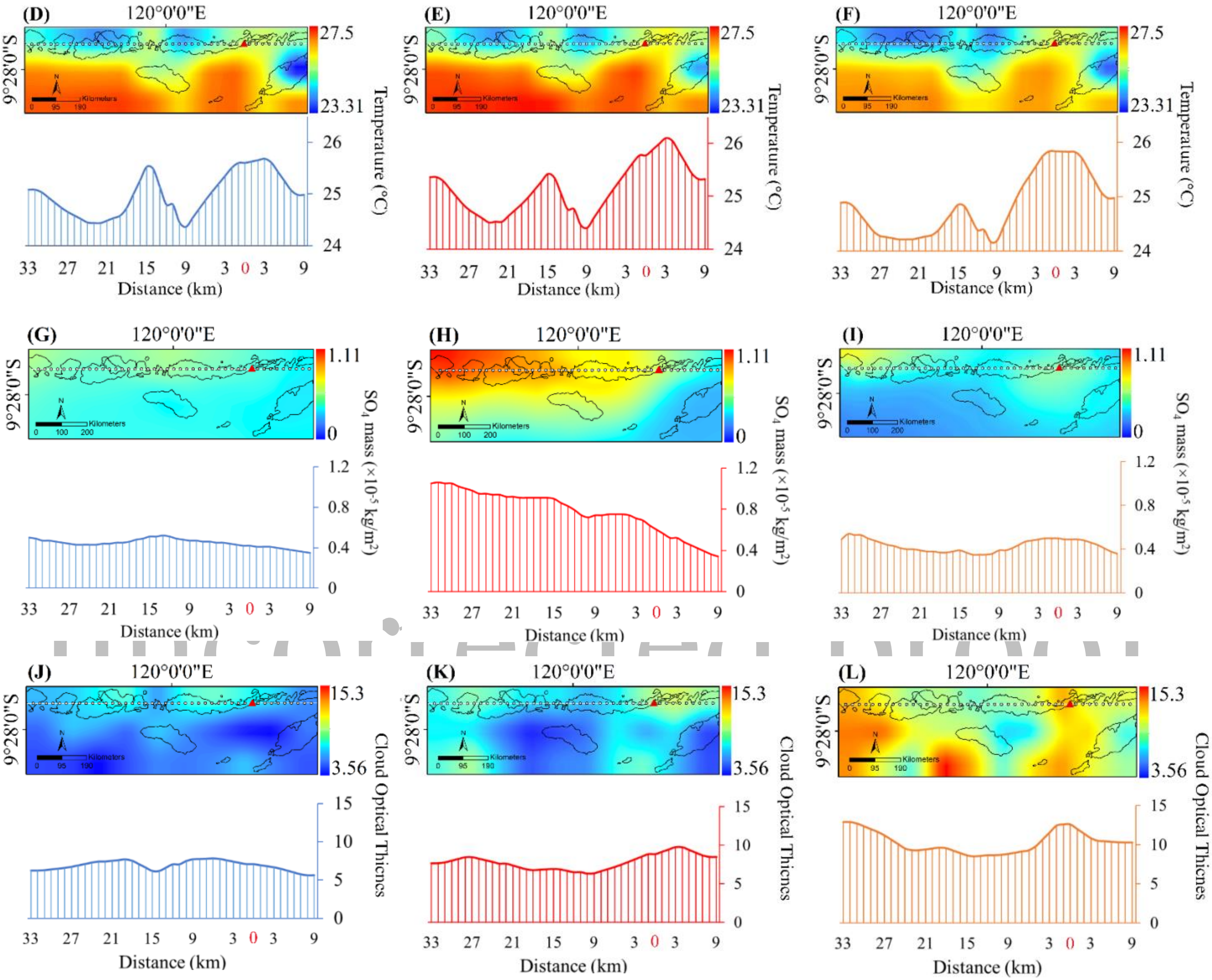
(D)
120°0'0"E
9°28'0"S
27.5
23.31
Temperature (°C)
26
25
24
33 27 21 15 9 3 0 3 9
Distance (km)
(E)
120°0'0"E
9°28'0"S
27.5
23.31
Temperature (°C)
26
25
24
33 27 21 15 9 3 0 3 9
Distance (km)
(F)
120°0'0"E
9°28'0"S
27.5
23.31
Temperature (°C)
26
25
24
33 27 21 15 9 3 0 3 9
Distance (km)
(G)
120°0'0"E
9°28'0"S
1.11
0
SO4 mass (×10-5 kg/m2)
1.2
0.8
0.4
0
33 27 21 15 9 3 0 3 9
Distance (km)
(H)
120°0'0"E
9°28'0"S
1.11
0
SO4 mass (×10-5 kg/m2)
1.2
0.8
0.4
0
33 27 21 15 9 3 0 3 9
Distance (km)
(I)
120°0'0"E
9°28'0"S
1.11
0
SO4 mass (×10-5 kg/m2)
1.2
0.8
0.4
0
33 27 21 15 9 3 0 3 9
Distance (km)
(J)
120°0'0"E
9°28'0"S
15.3
3.56
Cloud Optical Thicns
15
10
5
0
33 27 21 15 9 3 0 3 9
Distance (km)
(K)
120°0'0"E
9°28'0"S
15.3
3.56
Cloud Optical Thicns
15
10
5
0
33 27 21 15 9 3 0 3 9
Distance (km)
(L)
120°0'0"E
9°28'0"S
15.3
3.56
Cloud Optical Thicns
15
10
5
0
33 27 21 15 9 3 0 3 9
Distance (km)

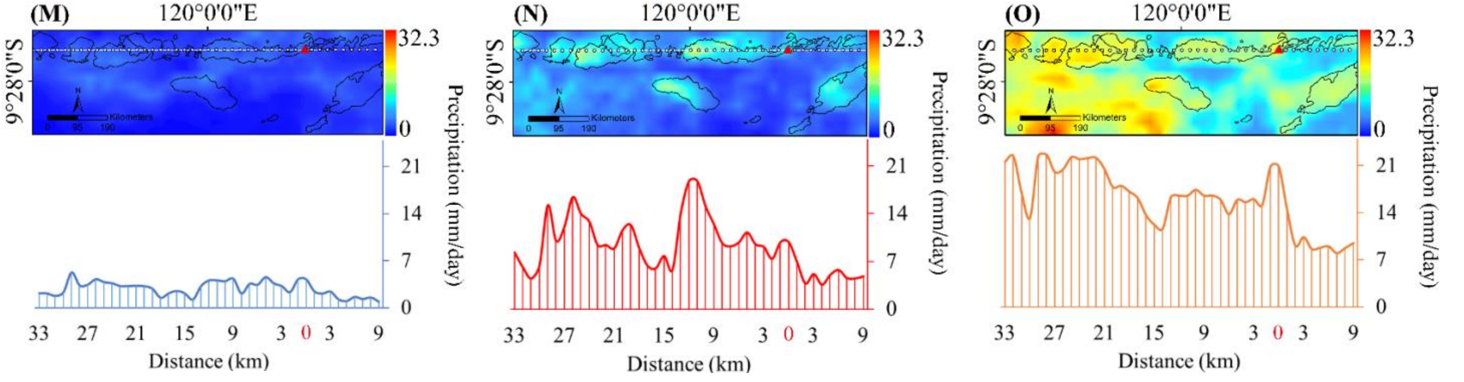

Figure 6. Spatiotemporal synthesis of atmospheric responses. The top panels of each sub-figure represent the monthly average spatial distribution, featuring a red triangle as the volcano location and a dotted line indicating the transect path. The bottoms panels display the corresponding monthly average longitudinal transects extending from the volcano location (0 km) to across the upwind and downwind sectors for October (baseline), November (syn-eruption), and December (post-eruption). The observed changes in the November and December phases correspond to the identified peak lags of SO_2 (1-day), SO_4 mass(16-day), Cloud Optical Thickness (21-day), and Precipitation (23-day), respectively.

5. Conclusions

The November 2024 eruption of Mount Lewotobi Laki-Laki triggereds a temporally and spatially phased series of atmospheric responses. The initial phase exhibited a brief warming of surface temperature (~27.6 °C) with a maximum correlation of r = 0.51 at a lag of 1 day, triggered by the Volcanic Blanket Effect, in which volcanic gases and ash absorb and trap Earth's radiation, resulting in localized warming. This effect is temporary, followed by gradual cooling (~25°C) as atmospheric reflectivity increases due to sulphate aerosol formation, consistent with the Volcanic Umbrella Effect. SO_2 reaches its highest correlation with sulphate aerosols, r = 0.62 at a lag of 16 days, reflecting gradual chemical conversion through atmospheric oxidation. Mature aerosols act as cloud condensation nuclei (CCN), enhancing COT with a peak correlation of r = 0.39 at a 21-day lag, making clouds more reflective and durable. The hydrological response appears to be the slowest, characterized by a two-phase pattern: initially suppressing precipitation during the degassing phase, then increasing to ~38 mm/day with a peak correlation of r = 0.55 at 23 days lag. Spatial analysis, conducted via longitudinal transects, reveals that these impacts are not stationary; rather, they follow a dominant East-to-West transport mechanism. While thermal anomalies were localized at the crater and extending up to 3 km eastward, the subsequent aerosol maturation and microphysical modifications triggered a "downwind shift" in precipitation following November's transport pathways. This process culminating in extreme rainfall in the distal downstream sectors (0-30 km) in December, rather than the immediate volcanic vicinity.

These findings confirm that aerosols modulate local weather through a sequence of rapid warming, atmospheric cooling, cloud modification, and delayed precipitation. Monitoring SO_2 and sulphate aerosols is therefore critical for supporting early warnings of extreme precipitation following eruptive surges. However, this study is limited by the lack of atmospheric vertical profile data and in situ validation, which prevents a complete understanding of altitude dynamics and cloud microphysical interactions. Consequently, further research should integrate WRF-Chem-based atmospheric modelling, multi-sensor satellite observations, and field measurements. The integration of these approaches, combined with longer observation periods, will also allow for advanced statistical verification such as the Granger causality test. Furthermore, future studies could explore the comparative impacts of subaerial and submarine eruptions, specifically how large-scale water vapor emissions in submarine events might influence the time-lag of sulphate formation and weather responses. This will enable aerosol, cloud, and precipitation feedback to be examined more comprehensively and improve the accuracy of volcanic weather impact predictions.

Author Contributions

Conceptualization, R.K., and S.R.; Methodology, R.K., and N.D.A.; Software, R.K.; Formal analysis, R.K., and C.W.L.; Investigation, R.K. and S.R.; Data curation, R.K. and A.S.; Validation, A.S., N.D.A., and C.W.L.; Resources, A.S. and N.D.A.; Writing original draft, R.K.; Writing review & editing, C.W.L., and N.D.A.; Visualization, R.K., and S.R.; Supervision, A.S. and N.D.A.; Project administration, A.S.; Funding acquisition, N.D.A, and A.S.

Acknowledgements

The authors express their sincere gratitude to the NASA Earth Science Data Systems (ESDS) for providing open-access satellite observations through the Giovanni platform, particularly from missions such as OMI, MODIS, MERRA-2, AIRS and GPM, which were essential for the atmospheric analysis in this study. Appreciation is also extended to the Center for Volcanology and Geological Hazard Mitigation (PVMBG) for publicly available eruption reports that supported contextual interpretation of the volcanic activity.

Data Availability

All raw satellite data utilized in this study (SO_2, sulphate aerosol concentrations, surface temperature, cloud optical thickness (COT), and precipitation) are publicly available through the NASA Goddard Earth Sciences Data and Information Services Center (GES DISC), accessed via the Giovanni platform (URL: https://giovanni.gsfc.nasa.gov/giovanni/). The processed and derived datasets generated in this research are available from the corresponding author upon reasonable request.

References

Amiot, C. G., Lang, T. J., Heever, S. C. Van Den, Ferrare, R. A., Sy, O. O., Carey, L. D., Christopher, S. A., Mecikalski, J. R., Freeman, S. W., Sokolowsky, G. A., Hostetler, C. A., & Tanelli, S. (2025). *Observed impacts of aerosol concentration on maritime tropical convection within constrained environments using airborne radiometer , radar , lidar , and dropsondes*. 12335–12355.

Arellano, S., Galle, B., Apaza, F., Avard, G., Barrington, C., Bobrowski, N., Bucarey, C., Burbano, V., Burton, M., & Chacón, Z. (2021). *Synoptic analysis of a decade of daily measurements of SO 2 emission in the troposphere from volcanoes of the global ground-based Network for Observation of Volcanic and Atmospheric Change*. 1167–1188.

Axebrink, E., Sporre, M. K., & Friberg, J. (2025). Impact of SO2 injection profiles on simulated volcanic forcing for the 2009 Sarychev eruptions - investigating the importance of using high-vertical-resolution methods when compiling SO2 data. *Atmospheric Chemistry and Physics*, *25*(4), 2047–2059. https://doi.org/10.5194/acp-25-2047-2025

Cai, Z., Griessbach, S., & Hoffmann, L. (2022). Improved estimation of volcanic SO2 injections from satellite retrievals and Lagrangian transport simulations: The 2019 Raikoke eruption. *Atmospheric Chemistry and Physics*, *22*(10), 6787–6809. https://doi.org/10.5194/acp-22-6787-2022

Ceppi, P., Brient, F., Zelinka, M. D., & Hartmann, D. L. (2017). Cloud feedback mechanisms and their representation in global climate models. *Wiley Interdisciplinary Reviews: Climate Change*, *8*(4). https://doi.org/10.1002/wcc.465

Chen, Y., Haywood, J., Wang, Y., Malavelle, F., Jordan, G., Peace, A., Partridge, D. G., Cho, N., Oreopoulos, L., Grosvenor, D., Field, P., Allan, R. P., & Lohmann, U. (2024). Substantial cooling effect from aerosol-induced increase in tropical marine cloud cover. *Nature Geoscience*, *17*(5), 404–410. https://doi.org/10.1038/s41561-024-01427-z

Global Volcanism Program. (2024). *Lewotobi (264180) in Volcanoes of the World, v. 5.2.3*. Smithsonian Institution.

Hagen, M., & Azevedo, A. (2023). Influence of Volcanic Activity on Weather and Climate Changes. *Atmospheric and Climate Sciences*, *13*(02), 138–158. https://doi.org/10.4236/acs.2023.132009

Haghighatnasab, M., Kretzschmar, J., Block, K., & Quaas, J. (2022). *Impact of Holuhraun volcano aerosols on clouds in cloud-system-resolving simulations*. 8457–8472.

Hall, R. (2012). Tectonophysics Late Jurassic – Cenozoic reconstructions of the Indonesian region and the Indian

Ocean. *Tectonophysics*, *570–571*, 1–41. https://doi.org/10.1016/j.tecto.2012.04.021

Hermanson, L., Bilbao, R., Dunstone, N., Ménégoz, M., Ortega, P., Timmreck, C., Yeager, S., & Danabasoglu, G. (2020). *Robust Multiyear Climate Impacts of Volcanic Eruptions in Decadal Prediction Systems Journal of Geophysical Research : Atmospheres*. https://doi.org/10.1029/2019JD031739

Hoffmann, L., Gilardi, L., Schmitz, M. T., Erbertseder, T., Bittner, M., Wüst, S., Schmid, M., & Rittweger, J. (2024). Investigating the spatiotemporal associations between meteorological conditions and air pollution in the federal state Baden - Württemberg (Germany). *Scientific Reports*, 1–16. https://doi.org/10.1038/s41598-024-56513-4

Lacis, A. A., Hansen, J. E., Russell, G. L., Oinas, V., & Jonas, J. (2013). The role of long-lived greenhouse gases as principal LW control knob that governs the global surface temperature for past and future climate change. *Tellus, Series B: Chemical and Physical Meteorology*, *65*(1), 1–25. https://doi.org/10.3402/tellusb.v65i0.19734

Li, Z., Lau, W. K. M., Ramanathan, V., Wu, G., Ding, Y., Manoj, M. G., Liu, J., Qian, Y., Li, J., Zhou, T., Fan, J., Rosenfeld, D., Ming, Y., Wang, Y., Huang, J., Wang, B., Xu, X., Lee, S. S., Cribb, M., … Brasseur, G. P. (2016). Aerosol and monsoon climate interactions over Asia. *Reviews of Geophysics*, *54*(4), 866–929. https://doi.org/10.1002/2015RG000500

Lin, C., Yu, J. Z., Lee, E., Chan, P. W., Ng, J. W. Y., Chan, Y. W., Zhang, T., Chen, Y., Chen, H., Zhang, Z., Chui, S. H. K., Fung, J. C. H., Liu, W., & Lau, A. K. H. (2025). Mysterious air pollution in south China linked to volcanic emissions from the Philippines. *Communications Earth and Environment*, *6*(1), 6–10. https://doi.org/10.1038/s43247-025-02073-y

Liu, X., Jeon, J., Nacht, A. R., & Larson, P. S. (2025). *Lag Associations of Precipitation and Temperature with Seven Types of Ambient Air Pollution Concentrations in the Midwestern United States : A Time Series Analysis with Seven Types of Ambient Air Pollution Concentrations in the Midwestern United States :* . 0–8. https://doi.org/10.20944/preprints202503.0438.v1

Mahrup, Ma'shum, M., & Fahrudin. (2021). Climate change in the Lesser Sunda Islands: The harsh region in the maritim continent of Indonesia. *IOP Conference Series: Earth and Environmental Science*, *824*(1). https://doi.org/10.1088/1755-1315/824/1/012115

Malavelle, F. F., Haywood, J. M., Jones, A., Gettelman, A., Clarisse, L., Bauduin, S., Allan, R. P., Karset, I. H. H., Kristjánsson, J. E., Oreopoulos, L., Cho, N., Lee, D., Bellouin, N., Boucher, O., Grosvenor, D. P., Carslaw, K. S., Dhomse, S., Mann, G. W., Schmidt, A., … Thordarson, T. (2017). Strong constraints on aerosol-cloud interactions from volcanic eruptions. *Nature*, *546*(7659), 485–491. https://doi.org/10.1038/nature22974

Marshall, L. R., Maters, E. C., Schmidt, A., Timmreck, C., Robock, A., & Toohey, M. (2022). Volcanic effects on climate: recent advances and future avenues. *Bulletin of Volcanology*, *84*(5). https://doi.org/10.1007/s00445-022-01559-3

Marshall, L. R., Smith, C. J., Forster, P. M., Aubry, T. J., Andrews, T., & Schmidt, A. (2020). Large Variations in Volcanic Aerosol Forcing Efficiency Due to Eruption Source Parameters and Rapid Adjustments. *Geophysical Research Letters*, *47*(19). https://doi.org/10.1029/2020GL090241

Ministry of Energy and Mineral Resources. (2024a). *Aktivitas Vulkanik Meningkat, PVMBG Naikkan Status G. Lewotobi Laki-laki Naik Jadi "AWAS."* https://www.esdm.go.id/id/media-center/arsip-berita/aktivitas-vulkanik-meningkat-pvmbg-naikkan-status-g-lewotobi-laki-laki-naik-jadi-awas?fbclid=IwY2xjawGVGbxleHRuA2FlbQIxMAABHTCZeDBpIpHCPLy-qwqC-9TsXknMdFqQi5PCUrutLIbXdsm9IOO5N7xgpg_aem_dLMg2xZ80VImL0bK6

Ministry of Energy and Mineral Resources. (2024b). *Badan Geologi: Erupsi G. Lewotobi Laki-Laki Keluarkan Gas SO2 Lebih dari 10.000 Ton per Hari*. https://www.esdm.go.id/en/media-center/news-archives/badan-geologi-erupsi-g-lewotobi-laki-laki-keluarkan-gas-so2-lebih-dari-10000-ton-per-hari

Nugroho, H. S., Asmoro, C. P., Achmad, A. R., Ardi, N. D., Wijaya, A. F. C., Utama, J. A., & Tayubi, Y. R. (2019). How tropical cyclones affected temperature, pressure, and humidity in Universitas Pendidikan Indonesia. *Journal of Physics: Conference Series*, *1280*(2). https://doi.org/10.1088/1742-6596/1280/2/022077

Paik, S., Min, S. K., Son, S. W., Lim, E. P., McGregor, S., An, S. Il, Kug, J. S., & Yeh, S. W. (2023). Impact of volcanic eruptions on extratropical atmospheric circulations: review, revisit and future directions. *Environmental Research Letters*, *18*(6). https://doi.org/10.1088/1748-9326/acd5e6

Papageorgiou, S. N. (2022). On correlation coefficients and their interpretation. *Journal of Orthodontics*, *49*(3), 359–361. https://doi.org/10.1177/14653125221076142

Reid, J. S., Maring, H. B., Narisma, G. T., Van Den Heever, S., Girolamo, L. Di, Ferrare, R., Lawson, P., Mace, G. G., Simpas, J. B., Tanelli, S., Ziemba, L., Van Diedenhoven, B., Bruintjes, R., Bucholtz, A., Flynn, C. B., Cambaliza, M. O., Chen, G., Diskin, G. S., Flynn, J. H., … Zavaleta, J. (2023). The Coupling Between Tropical Meteorology, Aerosol Lifecycle, Convection, and Radiation during the Cloud, Aerosol and Monsoon Processes Philippines Experiment (CAMP2Ex). *Bulletin of the American Meteorological Society*, *104*(6), E1179–E1205. https://doi.org/10.1175/BAMS-D-21-0285.1

Sadeghi, B., Crawford, A., Chai, T., Cohen, M., Sieglaff, J., Pavolonis, M., Kim, H. C., & Morris, G. (2025). Improving Volcanic SO2 Cloud Modeling Through Data Fusion and Trajectory Analysis: A Case Study of the 2022 Hunga Tonga Eruption. *Journal of Geophysical Research: Atmospheres*, *130*(4).

https://doi.org/10.1029/2024JD042421

Sahoo, S. S. (2024). Volcanic eruptions and climate: A complex interplay. *Journal of Geosciences Insights*, *2*(1), 25–28. https://doi.org/10.61577/jgi.2024.100005

Schallock, J., Brühl, C., Bingen, C., Höpfner, M., Rieger, L., & Lelieveld, J. (2023). Reconstructing volcanic radiative forcing since 1990, using a comprehensive emission inventory and spatially resolved sulfur injections from satellite data in a chemistry-climate model. *Atmospheric Chemistry and Physics*, *23*(2), 1169–1207. https://doi.org/10.5194/acp-23-1169-2023

Sellitto, P., Siddans, R., Belhadji, R., Carboni, E., Legras, B., Podglajen, A., Duchamp, C., & Kerridge, B. (2024). Observing the SO2 and Sulfate Aerosol Plumes From the 2022 Hunga Eruption With the Infrared Atmospheric Sounding Interferometer (IASI). *Geophysical Research Letters*, *51*(19). https://doi.org/10.1029/2023GL105565

Simanjuntak, F., & Lin, T. (2022). *Monsoon Effects on Chlorophyll-a , Sea Surface Temperature , and Ekman Dynamics Variability along the Southern Coast of Lesser Sunda Islands and Its Relation to ENSO and IOD Based on Satellite Observations*.

Stenchikov, G. (2009). The Role of Volcanic Activity in Climate and Global Change. In *Climate Change: Observed impacts on Planet Earth* (1st ed.). Elsevier B.V. https://doi.org/10.1016/B978-0-444-53301-2.00004-X

Stenchikov, G., Robock, A., Ramaswamy, V., Schwarzkopf, M. D., Hamilton, K., & Ramachandran, S. (2002). Arctic Oscillation response to the 1991 Mount Pinatubo eruption: Effects of volcanic aerosols and ozone depletion. *Journal of Geophysical Research Atmospheres*, *107*(24), ACL 28-1-ACL 28-16. https://doi.org/10.1029/2002JD002090

Su, T., Li, Z., Henao, N. R., Luan, Q., & Yu, F. (2024). Constraining effects of aerosol-cloud interaction by accounting for coupling between cloud and land surface. *Science Advances*, *10*(21), 1–9. https://doi.org/10.1126/sciadv.adl5044

Timmreck, C., Toohey, M., Zanchettin, D., Brönnimann, S., Lundstadt, E., & Wilson, R. (2021). The unidentified volcanic eruption of 1809: why it remains a climatic cold case. *Climate of the Past Discussions*, (April 1815), 1–39.

Toohey, M., Jia, Y., Tegetmeier, S., Toohey, M., Jia, Y., & Tegetmeier, S. (2021). Stratospheric residence time and the lifetime of volcanic aerosol. *Eguga*, EGU21-12131. https://ui.adsabs.harvard.edu/abs/2021EGUGA..2312131T/abstract

Trismidianto, Satiadi, D., Harjupa, W., Fathrio, I., Risyanto, Saufina, E., Muharsyah, R., Nuryanto, D. E., Nauval, F., Andarini, D. F., Purwaningsih, A., Harjana, T., Praja, A. S., Witono, A., Juaeni, I., & Suhandi, B. (2024).

Southerly Surge Impact on Rainfall Patterns in Southern Indonesia during Winter Monsoon and Madden–Julian Oscillation (MJO). *Atmosphere*, *15*(7). https://doi.org/10.3390/atmos15070840

Virtanen, A., Joutsensaari, J., Kokkola, H., Partridge, D. G., Blichner, S., Seland, Ø., Holopainen, E., Tovazzi, E., Lipponen, A., Mikkonen, S., Leskinen, A., Hyvärinen, A. P., Zieger, P., Krejci, R., Ekman, A. M. L., Riipinen, I., Quaas, J., & Romakkaniemi, S. (2025). High sensitivity of cloud formation to aerosol changes. *Nature Geoscience*, *18*(April). https://doi.org/10.1038/s41561-025-01662-y

Whitty, R. C. W., Ilyinskaya, E., Mason, E., Wieser, P. E., Liu, E. J., Schmidt, A., Roberts, T., Pfeffer, M. A., Brooks, B., Mather, T. A., Edmonds, M., Elias, T., Schneider, D. J., Oppenheimer, C., Dybwad, A., Nadeau, P. A., & Kern, C. (2020). Spatial and Temporal Variations in SO2 and PM2.5 Levels Around Kīlauea Volcano, Hawai'i During 2007–2018. *Frontiers in Earth Science*, *8*(May 2018). https://doi.org/10.3389/feart.2020.00036

Wirasatriya, A., Susanto, R. D., Kunarso, K., Jalil, A. R., Ramdani, F., & Puryajati, A. D. (2021). Northwest monsoon upwelling within the Indonesian seas. *International Journal of Remote Sensing*, *42*(14), 5437–5458. https://doi.org/10.1080/01431161.2021.1918790

Wong, A., Yim, W., Roy, I., & Roy, A. (2023). Can Volcanoes be Linked to Extreme Monsoon Rainfall in Asian Countries? *Asia Oceania Geosciences Society (AOGS) 20th Annual Meeting*. https://doi.org/10.13140/RG.2.2.26737.25446

Wong, A., Roy, I., Yim, W., & Roy, A. (2025). Volcanic eruptions as a cause of extreme weather with special focus on Hong Kong. In *Air Pollution and Related Health Risks* (pp. 331–350). Elsevier. https://doi.org/10.1016/B978-0-443-23965-6.00012-5

Wong, A., & Yim, W. (n.d.). *2021-2022 Tongan volcanic eruptions and record rainfall in eastern Australia and New Zealand*. Volcanoes Study Group, Hong Kong.

Yim, W. W.-S. (2005). The El Chichón eruption and rainfall distribution in Hong Kong during 1982. *Abstracts of the 5th Workshop of Asia-Pacific Space Geodynamics Program (APSG)*.

Yu, P., Portmann, R. W., Peng, Y., Liu, C. C., Zhu, Y., Asher, E., Bai, Z., Lu, Y., Bian, J., Mills, M., Schmidt, A., Rosenlof, K. H., & Toon, O. B. (2023). Radiative Forcing From the 2014–2022 Volcanic and Wildfire Injections. *Geophysical Research Letters*, *50*(13), 1–8. https://doi.org/10.1029/2023GL103791

Zheng, G., Su, H., Andreae, M. O., Pöschl, U., & Cheng, Y. (2024). Multiphase Buffering by Ammonia Sustains Sulfate Production in Atmospheric Aerosols. *AGU Advances*, *5*(4). https://doi.org/10.1029/2024AV001238